IEEE Access
Multidisciplinary Rapid Review Open Access Journal

Received August 27, 2020, accepted September 18, 2020, date of publication September 25, 2020, date of current version October 7, 2020.

Digital Object Identifier 10.1109/ACCESS.2020.3026676

Extreme Multistability in Simple Area-Preserving Map

HOUZHEN LI[1], (Graduate Student Member, IEEE), HAN BAO[1], LEI ZHU[2], BOCHENG BAO[1], (Member, IEEE), AND MO CHEN[1]

[1]School of Microelectronics and Control Engineering, Changzhou University, Changzhou 213164, China
[2]School of Electrical and Information Engineering, Jiangsu University of Technology, Changzhou 213001, China

Corresponding author: Bocheng Bao (mervinbao@126.com)

This work was supported in part by the National Natural Science Foundations of China under Grant 51777016 and Grant 61801054, in part by the Natural Science Foundation of Jiangsu Province, China, under Grant BK20191451, and in part by the Postgraduate Research and Practice Innovation Program of Jiangsu Province, China, under Grant KYCX20_2548.

ABSTRACT Initial condition-relied extreme multistability has been recently found in many continuous dynamical systems. However, such a specific phenomenon has not yet been discovered in a discrete iterative map. To investigate this phenomenon, this paper proposes a two-dimensional conservative map only with one sine nonlinearity. The proposed simple discrete map is area-preserving in the phase space and displays the coexistence of infinite chaotic and quasi-periodic orbits caused by infinite fixed points. Multiple numerical results indicate that the area-preserving chaotic and quasi-periodic orbits have the initial condition-relied quasi-periodic route to chaos and initial condition-boosting bifurcation dynamics, which allow the simple area-preserving map to emerge the complex phenomenon of extreme multistability. Furthermore, a microcontroller-based hardware platform is developed to implement the initial condition-boosting chaotic signals.

INDEX TERMS Area-preserving map, initial condition, extreme multistability, quasi-periodic route.

I. INTRODUCTION

Discrete iterative maps are closely associated with continuous-time dynamical flows arisen in physical problems [1]–[3]. In fact, discrete iterative map is a specific dynamical system with instant states described by continuous-time variables, which can seize the essential behavior of the dynamical flow. Despite the greater simplicity in their mathematical models, discrete iterative maps can also display chaotic behaviors [4]–[6], which are attracting much attention due to their engineering application merits [7]–[9].

Multistability has been revealed in physical and experimental dynamical systems as well as in pure mathematical models [10]. Multiple self-excited or hidden coexisting attractors with respective basins of attraction can be found in a variety of continuous ordinary differential systems [11], [12]. Recently, by designing the special equilibrium curves, several interesting multi-stable systems were developed and their coexisting convergent attractors were uncovered by Sambas *et al.* in [13]. Importantly, when the number of coexisting multiple attractors goes to infinity, such a coexistence phenomenon is defined as extreme multistability, which is closely relied on the initial conditions and has been reported in many continuous-time dynamical systems [14], [15]. Similarly, the phenomenon of multistability can be also observed in numerous discrete iterative maps of difference equations, including the kicked rotor map [2], bistable Hénon map [16], nonlinear hyperchaotic map [17], three-degree-of-freedom vibro-impact system [18], two-dimensional sine map with initials-boosted coexisting chaos [19], and two-dimensional memristive hyperchaotic maps [20]. However, such an initial condition-relied extreme multistability has not yet been found in a discrete iterative map.

Extreme multistability can be often encountered is some specific continuous-time dynamical systems. Because of the multi-stable line or plane equilibrium aroused by memristors, initial condition-relied extreme multistability with complex bifurcation routes was emerged in memristor-based chaotic circuits and systems [21]. By contrast, due to the infinitely many isolated equilibria caused by periodic nonlinearities, initial condition-boosting infinite attractors

The associate editor coordinating the review of this manuscript and approving it for publication was Ludovico Minati.

were found in some periodic function-based offset-boostable dynamical systems [22], [23]. Furthermore, by introducing a memristor with periodic memductance into an offset-boostable linear system, a new memristive chaotic system was presented [24], [25], from which extreme multistability with the initial condition-relied bifurcation route to chaos and boosting bifurcation dynamics were disclosed. Recently, a simple two-dimensional hyperchaotic discrete map was constructed by inducting sine nonlinearity, from which the initial condition-boosting bifurcation dynamics was reported [26]. Then, how to implement the initial condition-relied extreme multistabili-ty in a simple discrete iterative map? This paper will propose a simple area-preserving map, which can serve to exemplify the initial condition-relied extreme multistability.

Many important physical problems can be simplified into the solutions of conservative systems with two degrees of freedom, i.e. the solutions of discrete area-preserving maps of a two-dimensional domain onto itself [27]. Beyond their theoretical appeal, the discrete area-preserving maps play an important role in numerous engineering fields [28]. Thus, the understanding and interpretation is warranted to gain deeper insight into the fundamental natures of the considered phenomena. For the proposed simple area-preserving map, this paper will focus on its initial condition-relied bifurcation behaviors, involving the quasi-periodic route to chaos and boosting bifurcation dynamics.

The rest of this paper is structured as follows. Section II proposes a simple area-preserving map, and investigates its stability of infinite fixed points and parameter-dependent bifurcation behaviors. Section III studies extreme multistability with boosting bifurcation dynamics, including the initial condition-relied quasi-periodic route to chaos and initial condition-boosting bifurcation behaviors. Section IV develops a microcontroller-based hardware platform to implement the initial condition-boosting chaotic signals. Finally, Section V presents some conclusions.

II. PROPOSED SIMPLE AREA-PRESERVING MAP

This section proposes a simple area-preserving map, which is a two-dimensional discrete conservative chaotic map. The stability of infinite fixed points is analyzed. And then the parameter-dependent bifurcation behaviors are investigated.

A. MODEL DESCRIPTIONS

The simple area-preserving map is simplified from the Poincaré Map associated with the rotator state in the motion of a kicked rotator when the pivot is frictionless and only one periodic kick is considered [1], [2]. Without loss of generality, the proposed simple area-preserving map is mathematically modeled by

$$\begin{cases} x_{n+1} = x_n + a\sin(x_n + y_n) \\ y_{n+1} = x_n + y_n \end{cases} \tag{1}$$

where x_n and y_n represent two variables at discrete time n, and a is the only nonzero parameter. Thus, there is only one sine nonlinearity in the proposed map model. Besides, because of the odd symmetry of sine nonlinearity, the proposed map model has reflection symmetry $(x, y) \to (-x, -y)$, i.e. reflection about the origin (0, 0).

The map in (1) is area-preserving for any value of the nonzero parameter a, which can be proved by the determinant of its Jacobian matrix. The Jacobian matrix of the proposed map can be derived from (1) as

$$\boldsymbol{J} = \begin{bmatrix} 1 + a\cos(x_n + y_n) & a\cos(x_n + y_n) \\ 1 & 1 \end{bmatrix} \tag{2}$$

Obviously, the determinant of the above matrix can be obtained by

$$\det(\boldsymbol{J}) = 1 \tag{3}$$

Consequently, the dynamics of the proposed map is area-preserving [29], [30] and its phase space decreases to the surface of a torus [1], completely different from the dissipative map [26], [31].

B. INFINITE FIXED POINTS AND STABILITY

The stability of a discrete map involves its fixed point. The fixed point, denoted as $P = (x^*, y^*)$, of the simple area-preserving map in (1) is the real solution of the following equations

$$\begin{cases} x^* = x^* + a\sin(x^* + y^*) \\ y^* = x^* + y^* \end{cases} \tag{4}$$

Clearly, the fixed point can be expressed as

$$P = (x^*, y^*) = (0, m\pi) \tag{5}$$

where m is an integer number. Hence, the simple area-preserving map has the infinite fixed points with period π.

Substituting $x^* = 0$ and $y^* = m\pi$ into (2), the Jacobian matrix of the simple area-preserving map (1) at P is given by

$$\mathbf{J} = \begin{bmatrix} 1 + a\cos m\pi & a\cos m\pi \\ 1 & 1 \end{bmatrix} \tag{6}$$

Then, the corresponding characteristic polynomial is yielded as

$$\det(\mathbf{1}\lambda - \mathbf{J}) = \lambda^2 - (2 + a\cos m\pi)\lambda + 1 \tag{7}$$

The stability of P is analyzed by evaluating the eigenvalues of (7). Denote λ_1 and λ_2 as the two eigenvalues. If $|\lambda_1| < 1$ and $|\lambda_2| < 1$, the fixed point is asymptotically stable, whereas if $|\lambda_1| > 1$ or (and) $|\lambda_2| > 1$, the fixed point is unstable. From (7), the two eigenvalues are calculated as

$$\begin{aligned} \lambda_1 &= 1 + 0.5a\cos m\pi + \sqrt{(1 + 0.5a\cos m\pi)^2 - 1} \\ \lambda_2 &= 1 + 0.5a\cos m\pi - \sqrt{(1 + 0.5a\cos m\pi)^2 - 1} \end{aligned} \tag{8}$$

Clearly, two cases appear in (8), as follows:

Case I: $m = 2k$ (k is an integer).

There yields $\cos(m\pi) = 1$. The absolute values of two eigenvalues λ_1 and λ_2 related to the parameter a can be plotted in Fig. 1 (left). As can be observed, for $-4 \leq a \leq 0$,

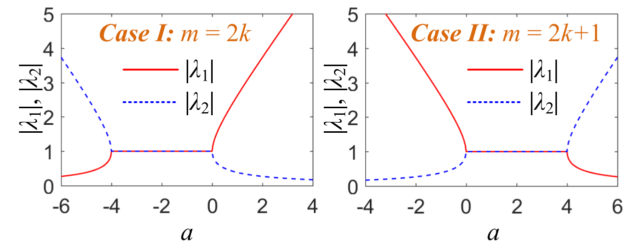

FIGURE 1. The absolute values of two eigenvalues λ_1 and λ_2 versus the parameter a.

the two eigenvalues λ_1 and λ_2 are always on the unit circle, i.e. $|\lambda_1| = |\lambda_2| = 1$, indicating that the fixed points are in critical states; for $a < -4$ and $a > 0$, one of the two eigenvalues λ_1 and λ_2 is always outside the unit circle, i.e. $|\lambda_1| > 1$ or $|\lambda_2| > 1$, resulting in that the fixed points are unstable.

Case II: $m = 2k + 1$ (k is an integer).

There obtains $\cos(m\pi) = -1$. The absolute values of two eigenvalues λ_1 and λ_2 related to the parameter a can be plotted in Fig. 1 (right). As can be seen, for $0 \leq a \leq 4$, the two eigenvalues λ_1 and λ_2 are always on the unit circle, i.e. $|\lambda_1| = |\lambda_2| = 1$, implying that the fixed points are in critical states; for $a < 0$ and $a > 4$, one of the two eigenvalues λ_1 and λ_2 is always outside the unit circle, i.e. $|\lambda_1| > 1$ or $|\lambda_2| > 1$, leading to that the fixed points are unstable.

Consequently, the proposed simple area-preserving map owns the infinite fixed points consisting of the critical points and unstable points.

C. QUASI-PERIODIC ROUTE TO CHAOS

Based on the discrete model of simple area-preserving map, the parameter-dependent bifurcation behaviors can be studied using the bifurcation diagrams, finite-time Lyapunov exponent (LE) spectra and phase portraits. Note that the finite-time LE spectra are calculated by employing the Wolf's Jacobian-based algorithm.

The first set of initial conditions and parameter interval are determined as $(x_0, y_0) = (-1, 0.8)$ and $a \in [-4, -0.5]$. The bifurcation diagrams and finite-time LEs (LE_1, LE_2) are simulated, as shown in Fig. 2(a), where the pink and dark-green trajectories in Fig. 2(a) (bottom) represent the bifurcation diagrams of the variables x and y respectively. As can be clearly seen, the largest LE_1 is positive in the parameter interval $[-2.3184, -2.2625]$ and the sum of two LEs is equal to zero, well demonstrating the existence of chaos and the conservation of map (1) [32].

The second set of initial conditions and parameter interval are conditionally selected as $(x_0, y_0) = (-1, 0.8-\pi)$ and $a \in [0.5, 4]$. Similarly, the bifurcation diagrams and finite-time LEs are simulated, as shown in Fig. 2(b), where the purple and regent-blue trajectories in Fig. 2(b) (bottom) stand for the bifurcation diagrams of the variables x and y respectively. Besides, the largest LE_1 is positive in the interval [2.2625, 2.3184] and the sum of two LEs equals zero. In particular,

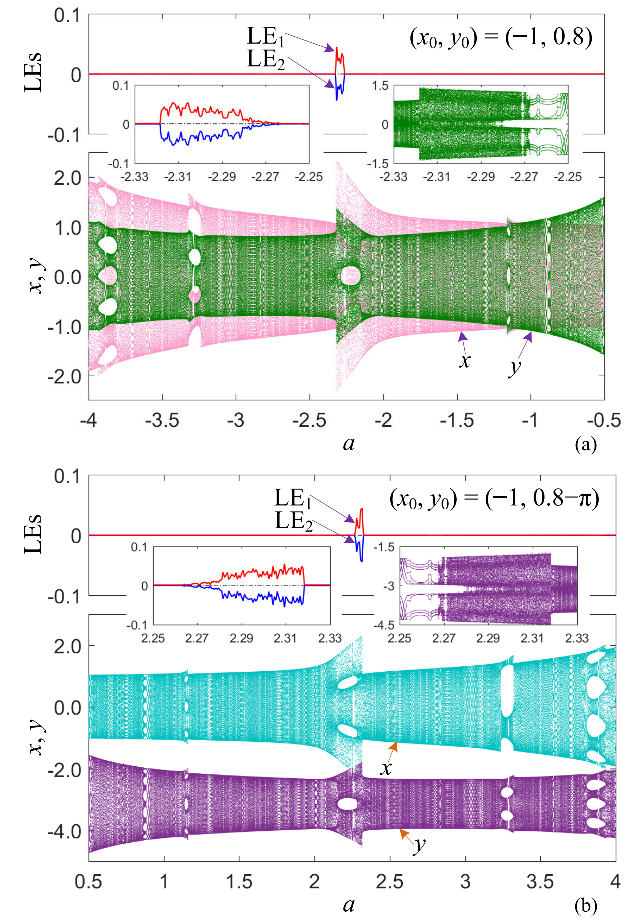

FIGURE 2. For two sets of initial conditions and parameter intervals, parameter-dependent bifurcation diagrams (bottom) and finite-time LEs (top) with the variations of the parameter a, where the partial enlarged drawings are embedded. (a) First set of $(x_0, y_0) = (-1, 0.8)$ and $a \in [-4, -0.5]$, (b) second set of $(x_0, y_0) = (-1, 0.8-\pi)$ and $a \in [0.5, 4]$.

the bifurcation behaviors disclosed in Fig. 2 have a nice symmetry in two symmetric parameter intervals, which just correspond to the two cases of infinite fixed points given in Fig. 1 as two sets of specific initial conditions are considered. But the difference is that the bifurcation diagram of the variable y in Fig. 2(b) is boosted by a $-\pi$ offset along the y-axis due to the occurrence of the $-\pi$ offset in the initial condition y_0.

The well-known Hénon map [33] undergoes the period-doubling route to chaos as its control parameters are changed, which is usually encountered in nonlinear continuous and discrete dynamical systems [34], [35]. In contrast, the minimal quadratic map reported by [36] goes through the quasi-periodic route to chaos with the increase of two control parameters. Therefore, similar to the results in [17], [36], the area-preserving chaotic orbit considered here is obtained from a quasi-periodic bifurcation scenario. Therefore, the proposed simple area-preserving map has a specific bifurcation route.

Based on the results in Fig. 2, the representative phase portraits of the simple area-preserving map for different symmetric parameters are simulated and depicted in Fig. 3, where

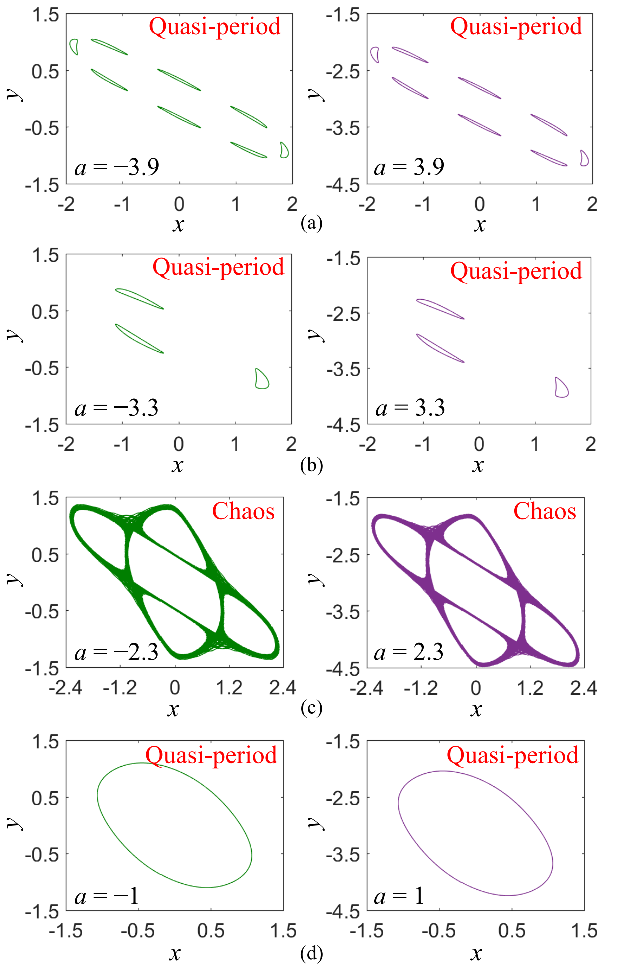

FIGURE 3. Representative phase portraits of simple area-preserving map for different symmetric parameters with two sets of initial conditions $(-1, 0.8)$ (left) and $(-1, 0.8-\pi)$ (right). (a) Quasi-period at $a = -3.9$ (left) and 3.9 (right), (b) quasi-period at $a = -3.3$ (left) and 3.3 (right), (c) chaos at $a = -2.3$ (left) and 2.3 (right), (d) quasi-period at $a = -1$ (left) and 1 (right).

the left and right drawings have the same topologies but with the $-\pi$ offset along the y-axis for the symmetric parameters. Here, Fig. 3(a) displays a quasi-periodic orbit with eight closed curves, Fig. 3(b) shows a quasi-periodic orbit with three closed curves, Fig. 3(c) reveals a chaotic orbit with complex fractal structure, and Fig. 3(d) exhibits a quasi-periodic orbit with one closed curve. Thus, the simple area-preserving map has only chaotic and quasi-periodic behaviors.

III. EXTREME MULTISTABILITY WITH BOOSTING BIFURCATIONS

Recently, there were many reports on the studies of extreme multistability closely related to the initial conditions. Memristor-based dynamical circuits and systems owning line or plane equilibrium can easily display the infinite coexisting attractors' behaviors of extreme multistability [14], [15], [37]. Therefore, to implement extreme multistability in discrete iterative maps is attracting. However, such discrete iterative maps were not reported previously.

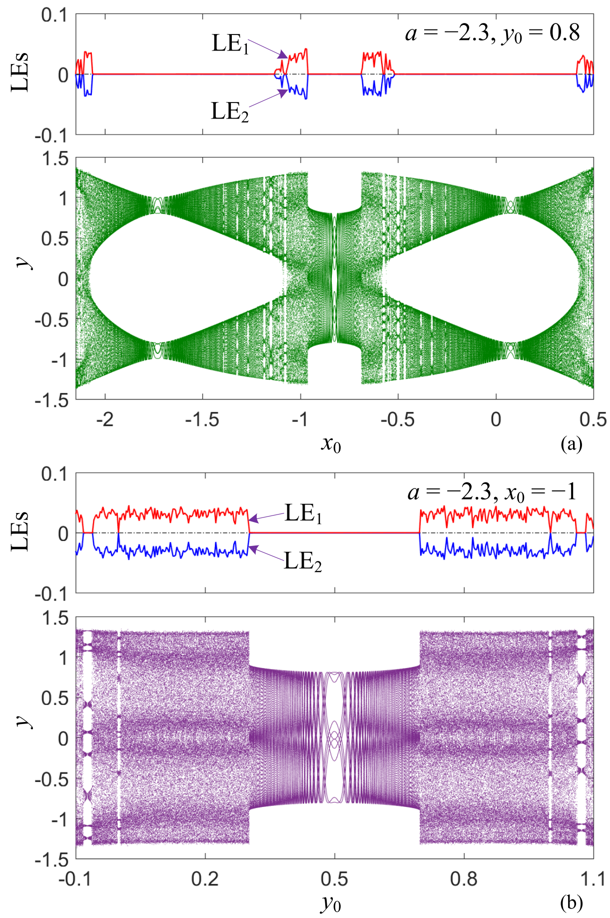

FIGURE 4. For fixed parameter $a = -2.3$, initial condition-relied bifurcation diagrams (bottom) and finite-time LEs (top) with the variations of the initial conditions, demonstrating the coexisting behaviors of infinite chaotic and quasi-periodic orbits. (a) $x_0 \in [-2.15, 0.5]$ with fixed $y_0 = 0.8$, (b) $y_0 \in [-0.1, 1.1]$ with fixed $x_0 = -1$.

A. COEXISTENCE OF INFINITE CHAOTIC AND QUASI-PERIODIC ORBITS

The map parameter is kept unchanged as $a = -2.3$. This subsection reveals the coexisting behaviors of infinite chaotic and quasi-periodic orbits by altering the initial conditions of map (1). Then, extreme multistability in the simple area-preserving map can be readily discussed.

Firstly, for fixed initial condition $y_0 = 0.8$, the initial condition x_0 is taken as a bifurcation parameter and varied in the initial interval $[-2.15, 0.5]$. The bifurcation diagram of the variable y and finite-time LEs are plotted in Fig. 4(a). Secondly, for fixed initial condition $x_0 = -1$, the initial condition y_0 is regarded as another bifurcation parameter and changed in the initial interval $[-0.1, 1.1]$. The bifurcation diagram of the variable y and finite-time LEs are depicted in Fig. 4(b). As can be seen, the specific quasi-periodic routes to chaos are observed as the two initial conditions x_0 and y_0 singly increase, leading to the coexistence of infinite chaotic and quasi-periodic orbits, i.e. the emergence of extreme multistability.

According to the bifurcation behaviors shown in Fig. 4, the striking phenomenon of extreme multistability can be

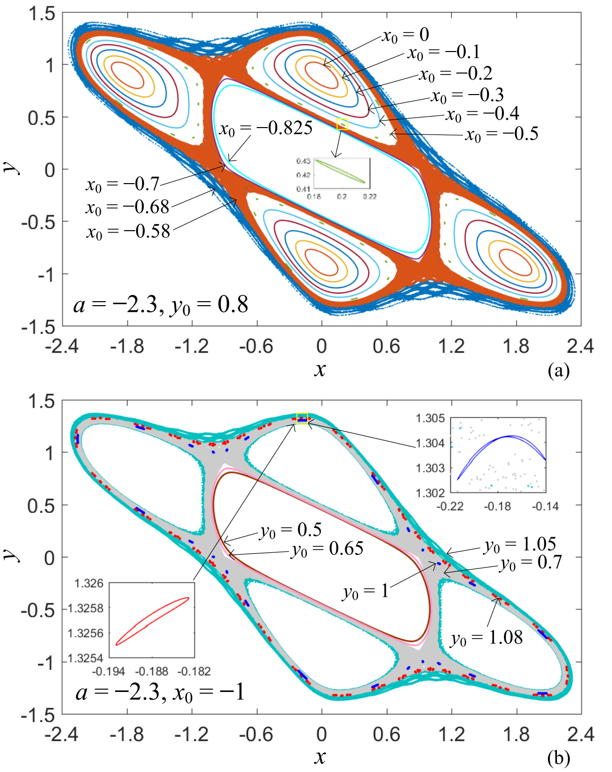

FIGURE 5. Descriptions of the coexisting chaotic and quasi-periodic orbits with different types, topologies and sizes. (a) Ten kinds of coexisting motions under different values of initial condition x_0 with fixed $y_0 = 0.8$, (b) six kinds of coexisting motions under different values of initial condition y_0 with fixed $x_0 = -1$.

intuitively demonstrated by some phase portraits of the coexisting chaotic and quasi-periodic orbits along the x_0- and y_0-axes. When ten values of initial condition x_0 are chosen, the phase portraits are together drawn in Fig. 5(a). By contrast, when six values of initial condition y_0 are determined, the phase portraits are together depicted in Fig. 5(b). Thus, the coexistence of infinite chaotic and quasi- periodic orbits with different types, topologies and sizes can be uncovered in such a simple area-preserving map. Note that in the phase portraits of Fig. 5, the seemingly discrete points and line segments are actually some independently closed tori with tiny sizes.

The Wolf's algorithm-based finite-time largest LE is an effectively indicator of chaos for a nonlinear dynamical system [19]. A colorful kinetic map can be depicted in the two-dimensional plane of initial conditions by computing the finite-time largest LE values of the simple area-preserving map, as shown in Fig. 6. The regions of initial conditions generating the trajectories with different largest LE values are painted by different colors. Magenta, red and yellow colors with positive values of largest LE refer to chaos regions, black with zero LE refers to quasi-period region, and white refers to the region at infinity. As can be observed from Fig. 6(a), the distribution image of chaos region resembles the representative chaotic orbit given in Fig. 5.

To further demonstrate the extreme multistability phenomenon, two sets of initial condition y_0-relied bifurcation

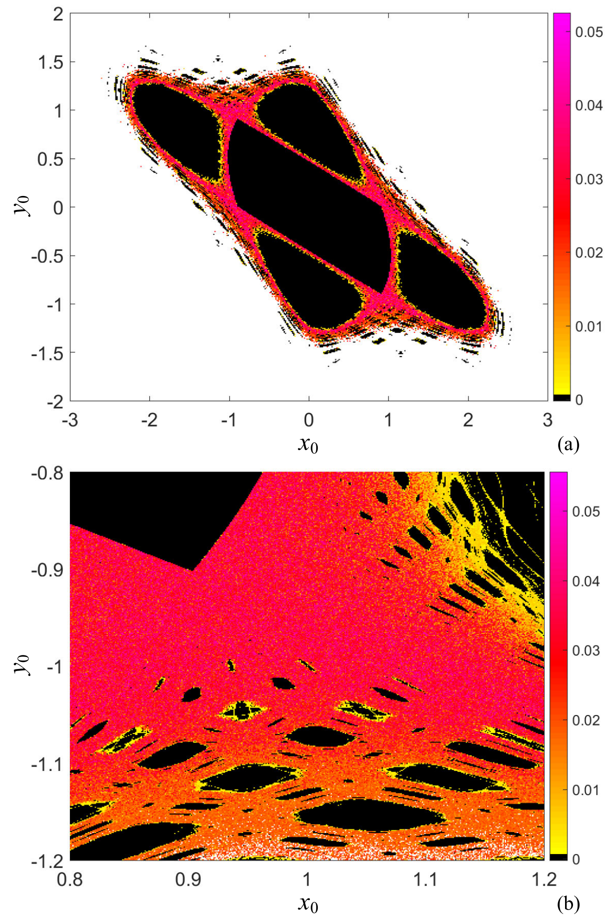

FIGURE 6. Kinetic maps in the x_0–y_0 initial plane that depicted by computing the finite-time largest LE values. (a) Full map in $x_0 \times y_0 \in [-3, 3]\times[-2, 2]$, (b) local map in $x_0 \times y_0 \in [0.8, 1.2]\times[-1.2, -0.8]$.

diagrams are supplemented in Fig. 7(a) through referring to the dynamical distributions in Fig. 6. Correspondingly, for the case in Fig. 7(a) (bottom) where $x_0 = 0$, when thirteen values of initial condition y_0 are determined, the phase portraits are concurrently drawn in Fig. 7(b), from which more unusual coexisting chaotic and quasi-periodic orbits are exhibited.

As shown in Fig. 4, the proposed simple area-preserving map possesses the specific quasi-periodic route to chaos closely relied on the initial conditions. And, most of all, it exhibits complex dynamical distribution in the x_0–y_0 initial plane given in Fig. 6. Therefore, it can be concluded that extreme multistability, i.e. the coexistence of infinite chaotic and quasi-periodic orbits, is emerged in the simple area-preserving map.

B. INITIAL CONDITION-BOOSTING DYNAMICS

Since the sine nonlinearity appeared in (1) is periodic with period 2π, the linear transformation $(x, y) \rightarrow (x, y + 2k\pi)$ (k is an integer) does not alter the map dynamics but gives rise to offset boosting along the y-axis with offset 2π [24], [38]. Thus, the proposed simple area-preserving map is an offset-boostable dynamical system, which allows the coexisting

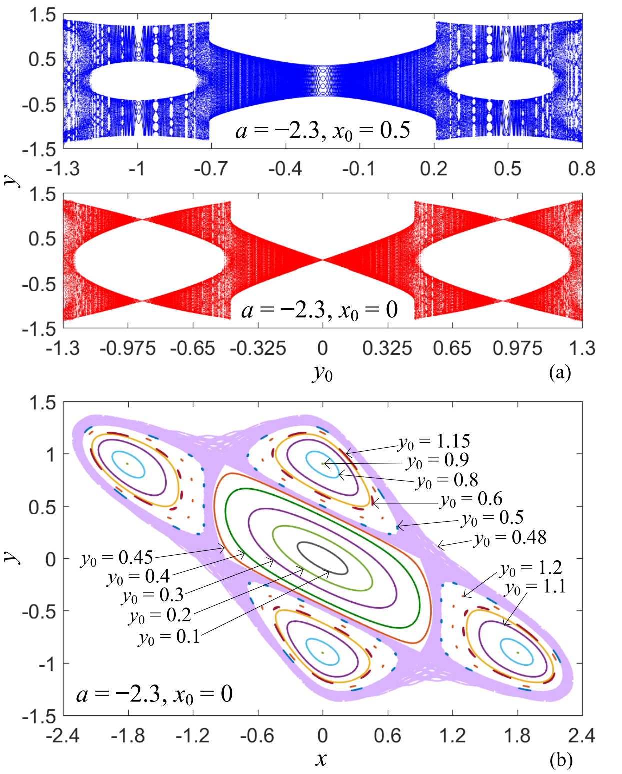

FIGURE 7. Initial condition-relied bifurcation diagrams as well as coexisting chaotic and quasi-periodic orbits. (a) The bifurcation diagrams versus the initial condition y_0 with fixed $x_0 = 0$ and $x_0 = 0.5$, (b) thirteen kinds of coexisting motions under different values of initial condition y_0 with fixed $x_0 = 0$.

bifurcation behaviors to be boosted by the initial condition y_0 along the y-axis [26].

Firstly, consider four values of initial condition y_0 as $y_0 = 0.8{+}2k\pi$ ($k = -1, 0, 1, 2$). When the initial condition x_0 is varied in the initial interval $[-2.15, 0.5]$, the bifurcation diagrams of the variable y are plotted in Fig. 8(a). Here, the colored trajectories are initiated from different values of initial condition y_0. Certainly, it can be found that the four bifurcation diagrams have an identical bifurcation structure, but each of them is boosted by a $2k\pi$ offset along the y-axis.

Secondly, take the value of initial condition x_0 as $x_0 = -1$. When the initial condition y_0 is varied in the respective initial intervals $[-0.1{+}2k\pi, 1.1{+}2k\pi]$ ($k = -1, 0, 1, 2$), the bifurca-tion diagrams of the variable y are plotted in Fig. 8(b). Here, the colored trajectories are initiated from different intervals of initial condition y_0. Thus, the four bifurcation diagrams in different initial intervals unfold the same bifurcation structure, but each of them can be boosted by the $2k\pi$ offset along the y-axis as well.

Corresponding to the results in Fig. 8, the coexisting kinetic maps boosted by the initial condition y_0 along the y-axis can be illustrated in Fig. 9(a), which well demonstrate that the initial condition-boosting bifurcation behaviors do exist in the proposed simple area-preserving map, similar to the initial-boosting plane bifurcation behaviors [24] but different from the initial-switched boosting attractors' behaviors [26].

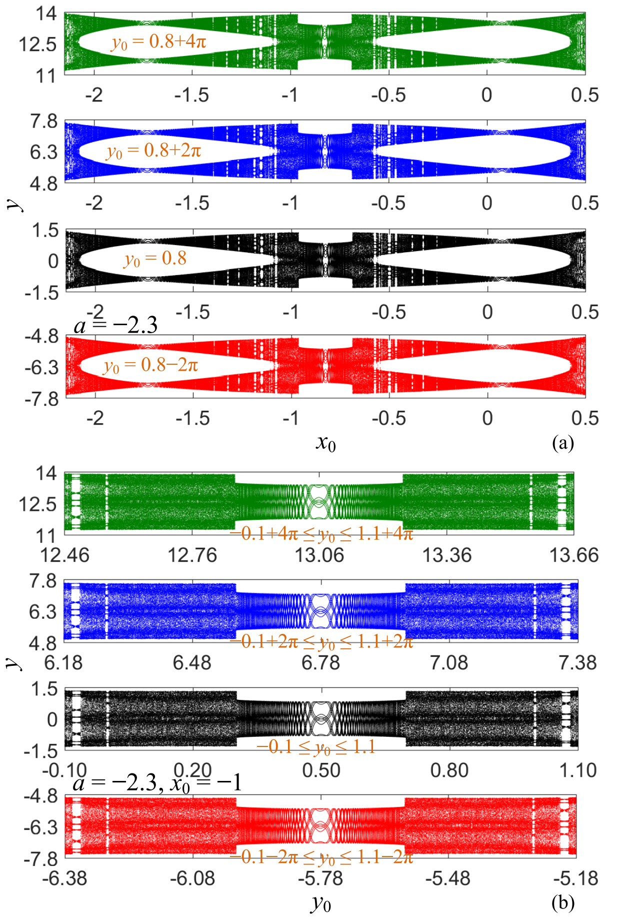

FIGURE 8. Initial condition y_0-boosted coexisting bifurcation behaviors along the y-axis. (a) For fixed $y_0 = 0.8{+}2k\pi$ ($k = -1, 0, 1, 2$), bifurcation diagrams as the initial condition x_0 increases in initial interval $[-2.15, 0.5]$, (b) for fixed $x_0 = -1$, bifurcation diagrams as the initial condition y_0 increases in four respective intervals $[-0.1{+}2k\pi, 1.1{+}2k\pi]$ ($k = -1, 0, 1, 2$).

In addition, four groups of initial condition settings are determined as $x_0 = -1$ and $y_0 = 0.8{+}2k\pi$ ($k = -1, 0, 1, 2$). The initial condition y_0-boosting chaotic sequences along the y-axis can be measured, as shown in Fig. 9(b). The results manifest that the chaotic sequences can be boosted in the dynamic amplitudes by the initial condition y_0 with period 2π, leading to the initial condition-boosting chaotic sequences.

The dynamical performances for the initial condition-boosting chaotic sequences of the simple area-preserving map can be evaluated through computing the largest finite-time LE_1, permutation entropy (PE) [39], spectral entropy (SE) [40], and Kaplan-Yorke dimension (D_{KY}) [19]. Thus, the numerical results for these four groups of chaotic sequences given in Fig. 9(b) are summarized in Table 1. Consequently, except for two sets of SEs for $(-1, 0.8)$ and $(-1, 0.8{+}2\pi)$ slightly lower than those for $(-1, 0.8{-}2\pi)$ and $(-1, 0.8{+}4\pi)$, the initial condition-boosting chaotic sequences have nearly the same performance indicators, indicating that the initial condition-boosting dynamics can implement the controllability of the oscillating amplitudes of chaotic sequences.

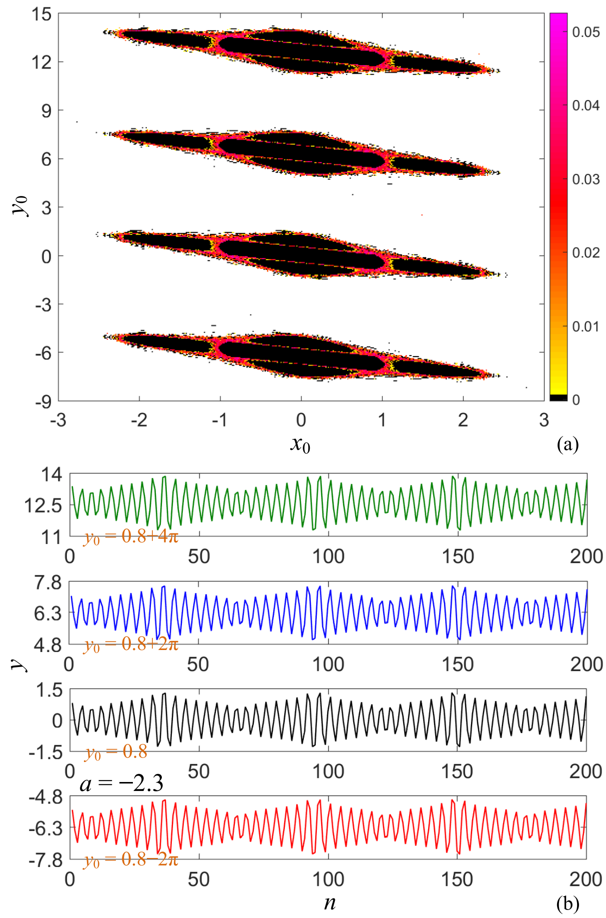

FIGURE 9. Initial condition y_0-boosted coexisting kinetic maps and chaotic sequences along the y-axis. (a) Coexisting kinetic maps in the x_0–y_0 initial plane, (b) coexisting chaotic sequences for fixed $x_0 = -1$ and $y_0 = 0.8+2k\pi$ ($k = -1, 0, 1, 2$).

TABLE 1. Performance evaluation for four groups of chaotic sequences.

(x_0, y_0)	LE_1	PE	SE	D_{KY}
$(-1, 0.8-2\pi)$	0.0370	3.3037	0.4346	2
$(-1, 0.8)$	0.0320	3.3429	0.2718	2
$(-1, 0.8+2\pi)$	0.0356	3.3417	0.2714	2
$(-1, 0.8+4\pi)$	0.0284	3.2884	0.4323	2

IV. HARDWARE PLATFORM FOR BOOSTING CHAOTIC SIGNALS

Based on a microcontroller, a programmable hardware experiment platform is developed. It mainly consists of MCU MSP430F149 (16-bit), D/A converter TLV5638 (12-bit), and peripheral circuit. The microcontroller implements the simple area-preserving map and two D/A converters generate four-channel analog voltage signals.

The parameter and initial conditions of the simple area-preserving map are assigned as $a = -2.3$, $x_0 = -1$ and $y_0 = 0.8+2k\pi$ ($k = -1, 0, 1, 2$). Preloading the parameter and initial conditions in the hardware device and running the map program using C language in the microcontroller, four-channel chaotic signals of the simple area-preserving map can be synchronously outputted and displayed on the digital oscilloscope.

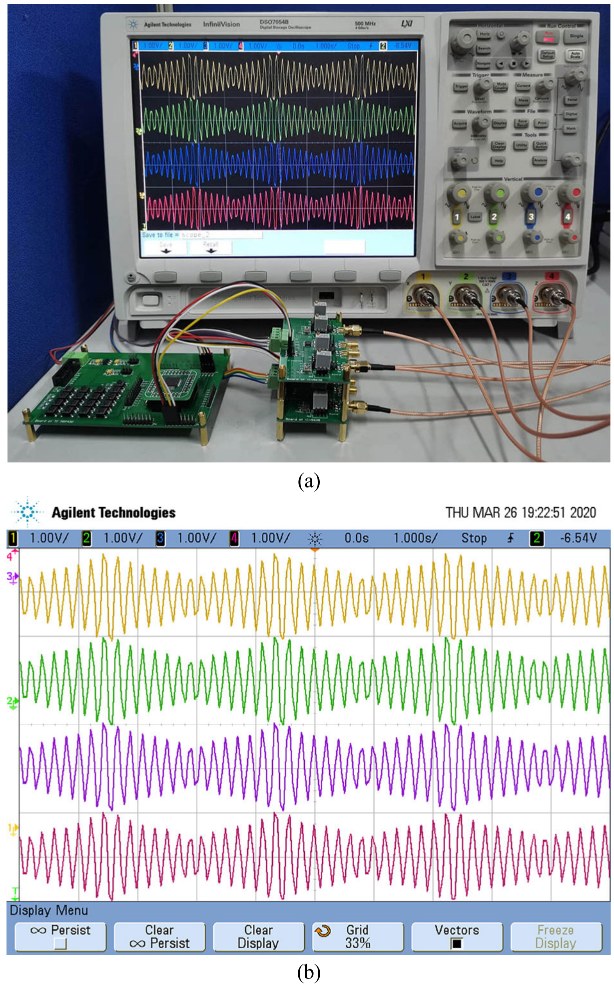

FIGURE 10. Hardware platform for generating multiple channel chaotic signals. (a) Hardware experimental prototype with the displayed chaotic signals, (b) four-channel initial condition-boosting chaotic signals captured from the hardware platform.

The hardware experimental prototype is snapshot in Fig. 10(a) and the four-channel initial condition-boosting chaotic signals are captured in Fig. 10(b). The experimental results show that four-channel initial condition-boosting chaotic signals synchronously output in the fixed amplitude ranges but with offset 2π, indicating the feasibility of the hardware implementation.

V. CONCLUSION

The coexistence phenomenon of extreme multistability relied on the initial conditions has been reported in many continuous dynamical systems. To study extreme multistability coexisted in a discrete iterative map, this paper proposed a simple area-preserving map. The area-preserving chaotic and quasi-periodic orbits have the initial condition-relied quasi-periodic route to chaos and initial condition-boosting bifurcation dynamics. These two characteristics allow the proposed simple area-preserving map to emerge extreme multistability.

The proposed simple area-preserving map had infinite fixed points consisting of the critical points and unstable points. The specific quasi-periodic route to chaos was explored through investigating the parameter and initial condition-relied dynamical behaviors. Particularly, the initial condition-relied extreme multistability with boosting bifurcation dynamics was uncovered using multiple numerical methods, and the initial condition-boosting chaotic sequences were thereby generated and captured from the microcontroller-based hardware platform. Of course, the simple area-preserving map could be applied to designing pseudorandom number generator with integrated circuit [41], which deserves further study.

REFERENCES

[1] P. A. Sousa-Silva and M. O. Terra, "Biparametric investigation of the general standard map: Multistability and global bifurcations," *Comput. Appl. Math.*, vol. 37, no. 3, pp. 3726–3743, Jul. 2018.

[2] L. C. Martins and J. A. C. Gallas, "Multistability, phase diagrams and statistical properties of the kicked rotor: A map with many coexisting attractors," *Int. J. Bifurcation Chaos*, vol. 18, no. 06, pp. 1705–1717, Jun. 2008.

[3] M.-F. Danca and M. Fečkan, "Hidden chaotic attractors and chaos suppression in an impulsive discrete economical supply and demand dynamical system," *Commun. Nonlinear Sci. Numer. Simul.*, vol. 74, pp. 1–13, Jul. 2019.

[4] X. Zhang and G. Chen, "Polynomial maps with hidden complex dynamics," *Discrete Continuous Dyn. Syst. B*, vol. 24, no. 6, pp. 2941–2954, 2019.

[5] F. A. Munir, M. Zia, and H. Mahmood, "Designing multi-dimensional logistic map with fixed-point finite precision," *Nonlinear Dyn.*, vol. 97, no. 4, pp. 2147–2158, Sep. 2019.

[6] S. Panahi, J. C. Sprott, and S. Jafari, "Two simplest quadratic chaotic maps without equilibrium," *Int. J. Bifurcation Chaos*, vol. 28, no. 12, Nov. 2018, Art. no. 1850144.

[7] C. Li, B. Feng, S. Li, J. Kurths, and G. Chen, "Dynamic analysis of digital chaotic maps via state-mapping networks," *IEEE Trans. Circuits Syst. I, Reg. Papers*, vol. 66, no. 6, pp. 2322–2335, Jun. 2019.

[8] D. Abbasinezhad-Mood and M. Nikooghadam, "Efficient anonymous password-authenticated key exchange protocol to read isolated smart meters by utilization of extended Chebyshev chaotic maps," *IEEE Trans. Ind. Informat.*, vol. 14, no. 11, pp. 4815–4828, Nov. 2018.

[9] C. Zhu and K. Sun, "Cryptanalyzing and improving a novel color image encryption algorithm using RT-enhanced chaotic tent maps," *IEEE Access*, vol. 6, pp. 18759–18770, 2018.

[10] A. N. Pisarchik and U. Feudel, "Control of multistability," *Phys. Rep.*, vol. 540, no. 4, pp. 167–218, Jul. 2014.

[11] P. R. Sharma, M. D. Shrimali, A. Prasad, N. V. Kuznetsov, and G. A. Leonov, "Control of multistability in hidden attractors," *Eur. Phys. J. Special Topics*, vol. 224, no. 8, pp. 1485–1491, Jul. 2015.

[12] N. Stankevich and E. Volkov, "Multistability in a three-dimensional oscillator: Tori, resonant cycles and chaos," *Nonlinear Dyn.*, vol. 94, no. 4, pp. 2455–2467, Dec. 2018.

[13] A. Sambas, S. Vaidyanathan, E. Tlelo-Cuautle, B. Abd-El-Atty, A. A. A. El-Latif, O. Guillén-Fernández, Sukono, Y. Hidayat, and G. Gundara, "A 3-D multi-stable system with a peanut-shaped equilibrium curve: Circuit design, FPGA realization, and an application to image encryption," *IEEE Access*, vol. 8, pp. 137116–137132, 2020.

[14] B.-C. Bao, Q. Xu, H. Bao, and M. Chen, "Extreme multistability in a memristive circuit," *Electron. Lett.*, vol. 52, no. 12, pp. 1008–1010, Jun. 2016.

[15] H. Bao, N. Wang, B. Bao, M. Chen, P. Jin, and G. Wang, "Initial condition-dependent dynamics and transient period in memristor-based hypogenetic jerk system with four line equilibria," *Commun. Nonlinear Sci. Numer. Simul.*, vol. 57, pp. 264–275, Apr. 2018.

[16] G. A. Casas and P. C. Rech, "Multistability annihilation in the Hénon map through parameters modulation," *Commun. Nonlinear Sci. Numer. Simul.*, vol. 17, no. 6, pp. 2570–2578, Jun. 2012.

[17] H. Natiq, S. Banerjee, M. R. K. Ariffin, and M. R. M. Said, "Can hyperchaotic maps with high complexity produce multistability?" *Chaos, Interdiscipl. J. Nonlinear Sci.*, vol. 29, no. 1, Jan. 2019, Art. no. 011103.

[18] Y. Zhang and G. Luo, "Multistability of a three-degree-of-freedom vibro-impact system," *Commun. Nonlinear Sci. Numer. Simul.*, vol. 57, pp. 331–341, Apr. 2018.

[19] H. Bao, Z. Hua, N. Wang, L. Zhu, M. Chen, and B.-C. Bao, "Initials-boosted coexisting chaos in a 2D sine map and its hardware implementation," *IEEE Trans. Ind. Informat.*, early access, May 4, 2020, doi: 10.1109/TII.2020.2992438.

[20] H. Li, Z. Hua, H. Bao, L. Zhu, M. Chen, and B. Bao, "Two-dimensional memristive hyperchaotic maps and application in secure communication," *IEEE Trans. Ind. Electron.*, early access, Sep. 15, 2020, doi: 10.1109/TIE.2020.3022539.

[21] M. Chen, M. Sun, H. Bao, Y. Hu, and B. Bao, "Flux–Charge analysis of two-memristor-based Chua's circuit: Dimensionality decreasing model for detecting extreme multistability," *IEEE Trans. Ind. Electron.*, vol. 67, no. 3, pp. 2197–2206, Mar. 2020.

[22] C. Li and J. C. Sprott, "An infinite 3-D quasiperiodic lattice of chaotic attractors," *Phys. Lett. A*, vol. 382, no. 8, pp. 581–587, Feb. 2018.

[23] Q. Lai, C. Chen, X.-W. Zhao, J. Kengne, and C. Volos, "Constructing chaotic system with multiple coexisting attractors," *IEEE Access*, vol. 7, pp. 24051–24056, 2019.

[24] H. Bao, M. Chen, H. Wu, and B. Bao, "Memristor initial-boosted coexisting plane bifurcations and its extreme multi-stability reconstitution in two-memristor-based dynamical system," *Sci. China Technol. Sci.*, vol. 63, no. 4, pp. 603–613, Apr. 2020.

[25] M. Chen, X. Ren, H. G. Wu, Q. Xu, and B. C. Bao, "Periodically varied initial offset boosting behaviors in a memristive system with cosine memductance," *Frontiers Inform. Technol. Electron. Eng.*, vol. 20, no. 12, pp. 1706–1716, Dec. 2019.

[26] B. C. Bao, H. Z. Li, L. Zhu, X. Zhang, and M. Chen, "Initial-switched boosting bifurcations in 2D hyperchaotic map," *Chaos, Interdiscipl. J. Nonlinear Sci.*, vol. 30, no. 3, Mar. 2020, Art. no. 033107.

[27] M. Hénon, "Numerical study of quadratic area-preserving mappings," *Quart. Appl. Math.*, vol. 27, no. 3, pp. 291–312, Oct. 1969.

[28] X. Tricoche, C. Garth, and A. Sanderson, "Visualization of topological structures in area-preserving maps," *IEEE Trans. Vis. Comput. Graphics*, vol. 17, no. 12, pp. 1765–1774, Dec. 2011.

[29] Z. H. Liu and S. G. Chen, "Synchronization of a conservative map," *Phys. Rev. E, Stat. Phys. Plasmas Fluids Relat. Interdiscip. Top.*, vol. 56, no. 2, pp. 1585–1589, Aug. 1997.

[30] S. Mahata, S. Das, and N. Gupte, "Synchronization in area-preserving maps: Effects of mixed phase space and coherent structures," *Phys. Rev. E, Stat. Phys. Plasmas Fluids Relat. Interdiscip. Top.*, vol. 93, no. 6, Jun. 2016, Art. no. 062212.

[31] Z. Elhadj and J. C. Sprott, "On the dynamics of A new simple 2-d rational discrete mapping," *Int. J. Bifurcation Chaos*, vol. 21, no. 01, pp. 155–160, Jan. 2011.

[32] N. Wang, G. Zhang, and H. Bao, "Infinitely many coexisting conservative flows in a 4D conservative system inspired by LC circuit," *Nonlinear Dyn.*, vol. 99, no. 4, pp. 3197–3216, Mar. 2020.

[33] M. Hénon, "A two-dimensional mapping with a strange attractor," *Commun. Math. Phys.*, vol. 50, no. 1, pp. 69–77, Feb. 1976.

[34] S. Jafari, V. T. Pham, S. M. R. H. Golpayegani, M. Moghtadaei, and S. T. Kingni, "The relationship between chaotic maps and some chaotic systems with hidden attractors," *Int. J. Bifurc. Chaos*, vol. 26, no. 13, Dec. 2016, Art. no. 1650211.

[35] B. Bao, J. Luo, H. Bao, C. Chen, H. Wu, and Q. Xu, "A simple nonautonomous hidden chaotic system with a switchable stable node-focus," *Int. J. Bifurcation Chaos*, vol. 29, no. 12, Nov. 2019, Art. no. 1950168.

[36] Z. Elhadj and J. C. Sprott, "A minimal 2-D quadratic map with quasi-periodic route to chaos," *Int. J. Bifurcation Chaos*, vol. 18, no. 5, pp. 1567–1577, May 2008.

[37] B. Bao, T. Jiang, G. Wang, P. Jin, H. Bao, and M. Chen, "Two-memristor-based Chua's hyperchaotic circuit with plane equilibrium and its extreme multistability," *Nonlinear Dyn.*, vol. 89, no. 2, pp. 1157–1171, 2017.

[38] C. B. Li, J. C. Sprott, and Y. Mei, "An infinite 2-D lattice of strange attractors," *Nonlinear Dyn.*, vol. 89, no. 4, pp. 2629–2639, Sep. 2017.

[39] C. Bandt and B. Pompe, "Permutation entropy: A natural complexity measure for time series," *Phys. Rev. Lett.*, vol. 88, no. 17, Apr. 2002, Art. no. 174102.

[40] H. Bao, W. Liu, and M. Chen, "Hidden extreme multistability and dimensionality reduction analysis for an improved non-autonomous memristive FitzHugh–Nagumo circuit," *Nonlinear Dyn.*, vol. 96, no. 3, pp. 1879–1894, May 2019.
[41] Z. Y. Hua, Y. C. Zhou, and B. C. Bao, "Two-dimensional sine chaotification system with hardware implementation," *IEEE Trans. Ind. Informat.*, vol. 16, no. 2, pp. 887–897, Feb. 2020.

HOUZHEN LI (Graduate Student Member, IEEE) received the B.S. degree in optoelectronic information science and engineering from the Changshu Institute of Technology, Suzhou, China, in 2019. He is currently pursuing the M.S. degree in electronics science and technology with the School of Microelectronics and Control Engineering, Changzhou University, Changzhou, China. His research interests include memristive neuromorphic circuit, and nonlinear circuits and systems.

HAN BAO received the B.S. degree in landscape design from the Finance and Economics University of Jiangxi, Nanchang, China, in 2015, and the M.S. degree in art and design from Changzhou University, Changzhou, China, in 2018. He is currently pursuing the Ph.D. degree in nonlinear system analysis and measurement technology with the Nanjing University of Aeronautics and Astronautics, Nanjing, China. In 2019, he visited the Computer Science Department, University of Auckland, New Zealand. His research interests include memristive neuromorphic circuit, nonlinear circuits and systems, and artificial intelligence.

LEI ZHU received the B.S. degree in mechanical engineering from Yangzhou University, Yangzhou, China, in 2002, and the M.S. degree in optical engineering from Yanshan University, Qinhuangdao, China, in 2006. He is currently an Associate Professor with the School of Electrical and Information Engineering, Jiangsu University of Technology, Changzhou, China. His research interest mainly focuses on nonlinear circuits and systems.

BOCHENG BAO (Member, IEEE) received the B.S. and M.S. degrees in electronic engineering from the University of Electronics Science and Technology of China, Chengdu, China, in 1986 and 1989, respectively, and the Ph.D. degree in information and communication engineering from the Nanjing University of Science and Technology, Nanjing, China, in 2010.

He has more than 20 years' experience in the industry and was with several enterprises as Senior Engineer and the General Manager. From 2008 to 2011, he was a Professor with the School of Electrical and Information Engineering, Jiangsu University of Technology, Changzhou, China. Then, he was a Full Professor with the School of Microelectronics and Control Engineering, Changzhou University, Changzhou, China. In 2013, he visited the Department of Electrical and Computer Engineering, University of Calgary, Calgary, AB, Canada. His research interests include bifurcation and chaos, analysis and simulation in neuromorphic circuits, power electronic circuits, and nonlinear circuits and systems.

Dr. Bao was a recipient of The IET Premium awards in 2018.

MO CHEN received the B.S. degree in information engineering, the M.S. degree in electromagnetic field and microwave technology, and the Ph.D. degree in electromagnetic field and microwave technology from Southeast University, Jiangsu, China, in 2003, 2006, and 2009, respectively.

From 2009 to 2013, she was a Lecturer with Southeast University. She is currently an Associate Professor with the School of Microelectronics and Control Engineering, Changzhou University, Changzhou, China. Her research interests include memristor and its application circuits, and other nonlinear circuits and systems.